

Chapman University

Chapman University Digital Commons

Biology, Chemistry, and Environmental Sciences Faculty Articles and Research Science and Technology Faculty Articles and Research

2-18-2019

Phylogenetic and Biogeographic Controls of Plant Nighttime Stomatal Conductance


Kailiang Yu
University of Utah

Gregory R. Goldsmith
Chapman University, goldsmi@chapman.edu

Yujie Wang
University of Utah

William R. L. Anderegg
University of Utah

Follow this and additional works at: https://digitalcommons.chapman.edu/sees_articles

 Part of the [Forest Biology Commons](#), [Other Forestry and Forest Sciences Commons](#), [Other Life Sciences Commons](#), [Other Plant Sciences Commons](#), and the [Plant Biology Commons](#)

Recommended Citation

Yu K, Goldsmith GR, Wang Y, Anderegg WRL. 2019. Phylogenetic and biogeographic controls of plant nighttime stomatal conductance. *New Phytologist*, 222, 4, (1778-1788), (2019). <https://doi.org/10.1111/nph.15755>

This Article is brought to you for free and open access by the Science and Technology Faculty Articles and Research at Chapman University Digital Commons. It has been accepted for inclusion in Biology, Chemistry, and Environmental Sciences Faculty Articles and Research by an authorized administrator of Chapman University Digital Commons. For more information, please contact laughtin@chapman.edu.

Phylogenetic and Biogeographic Controls of Plant Nighttime Stomatal Conductance

Comments

This is the accepted version of the following article:

Yu K, Goldsmith GR, Wang Y, Anderegg WRL. 2019. Phylogenetic and biogeographic controls of plant nighttime stomatal conductance. *New Phytologist*, 222, 4, (1778-1788), (2019). <https://doi.org/10.1111/nph.15755>

which has been published in final form at <https://doi.org/10.1111/nph.15755>. This article may be used for non-commercial purposes in accordance with [Wiley Terms and Conditions for Self-Archiving](#).

Copyright

Wiley

Phylogenetic and biogeographic controls of plant nighttime stomatal conductance

Kailiang Yu^{1*}, Gregory R. Goldsmith², Yujie Wang¹, William R. L. Anderegg¹

¹*School of Biological Sciences, University of Utah, Salt Lake City, UT 84112, USA*

²*Schmid College of Science and Technology, Chapman University, Orange, CA 92866, USA*

Correspondence: Kailiang Yu, email: ky9hc@virginia.edu; Telephone: +41795926975

Received: 19 December 2018

Accepted: 3 February 2019

ORCID ID, Kailiang Yu: <https://orcid.org/0000-0003-4223-5169>

Gregory R. Goldsmith: <https://orcid.org/0000-0003-3567-8949>

Yujie Wang: <https://orcid.org/0000-0002-3729-2743>

William R. L. Anderegg: <https://orcid.org/0000-0001-6551-3331>

This article has been accepted for publication and undergone full peer review but has not been through the copyediting, typesetting, pagination and proofreading process, which may lead to differences between this version and the Version of Record. Please cite this article as doi: 10.1111/nph.15755

This article is protected by copyright. All rights reserved.

Summary

- The widely documented phenomenon of nighttime stomatal conductance (g_{sn}) could lead to substantial water loss with no carbon gain, and thus it remains unclear whether nighttime stomatal conductance confers a functional advantage. Given that studies of g_{sn} have focused on controlled environments or small numbers of species in natural environments, a broad phylogenetic and biogeographic context could provide insights into potential adaptive benefits of g_{sn} .
- We measured g_{sn} on a diverse suite of species ($n = 73$) across various functional groups and climates-of-origin in a common garden to study the phylogenetic and biogeographic/climatic controls on g_{sn} and further assessed the degree to which g_{sn} co-varied with leaf functional traits and daytime gas exchange rates.
- Closely related species were more similar in g_{sn} than expected by chance. Herbaceous species had higher g_{sn} than woody species. Species that typically grow in climates with lower mean annual precipitation – where the fitness cost of water loss should be the highest – generally had higher g_{sn} .
- Our results reveal the highest g_{sn} rates in species from environments where neighboring plants compete most strongly for water, suggesting a possible role for the competitive advantage of g_{sn} .

Key Words

Stomata, gas exchange, transpiration, ecosystem flux, phylogenetic, biogeographic, adaption.

INTRODUCTION

Plants capture atmospheric CO_2 for photosynthesis and lose water vapor through stomatal pores on leaves. Thus, stomata strongly influence the carbon and water fluxes of terrestrial ecosystems and modeling stomatal behavior is essential for projections of climate impacts on ecosystems, land-atmosphere interactions, and carbon cycle feedbacks (Berry *et al.* 2010; Jasechko *et al.* 2013; Franks *et al.* 2017; Anderegg *et al.* 2018). A broad body of research has examined how stomatal conductance during the day responds to genetic controls and/or environmental conditions (Buckley, 2005; McAdam & Brodribb, 2015; Brodribb & McAdam, 2017). However, it is well established that many plants continue to lose water at night. In particular, there is extensive evidence of significant nighttime stomatal conductance (g_{sn}) and transpiration (E_n) in a diverse range of C_3 and C_4 plants across various habits and in multiple climate zones (Snyder *et al.* 2003; Daley & Phillips, 2006; Caird *et al.* 2007; Dawson *et al.* 2007; Phillips *et al.* 2010; Ogle *et al.* 2012; Hoshika *et al.*

2018). These observations are at odds with optimal stomata theories, which suggest that C_3 and C_4 plants should close stomata completely to avoid water loss when there is no carbon gain and little need to cool leaves during the night (Snyder *et al.* 2003; Caird *et al.* 2007).

E_n typically ranges from 10% to 15% of daytime rates, and can reach up to 20-30% of daytime rates (Bucci *et al.* 2004; Caird *et al.* 2007; Sellin & Lubenets, 2010; Ogle *et al.* 2012). This is a substantial water flux, especially for plants in dry regions where growth is often water limited (Yu *et al.*, 2016; Chen *et al.*, 2018). Previous studies have mainly used sap flow sensors to measure E_n at tree individual scales (Daley & Phillips, 2006; Caird *et al.* 2007; Dawson *et al.* 2007). This method, however, does not allow for the direct measurements of g_{sn} . Sapflow also does not generally partition recharge of plant water storage and E_n and therefore could overestimate the magnitude of E_n . Quantification of E_n at large scales remains difficult because of the technical obstacles in using eddy flux tower and remote sensing data during the nighttime (De Dios *et al.*, 2015). However, in the few instances where quantification has been attempted, E_n has been found to be significant (8-9% of daytime transpiration) (Novick *et al.* 2009). Most large-scale ecosystem models either ignore nighttime water loss or set a low and constant value of g_{sn} or E_n , which can lead to large biases in the estimates of plant water-use efficiency, ecosystem transpiration, and ecosystem carbon/water cycling in a changing climate (Novick *et al.* 2009; Zeppel *et al.* 2014; De Dios *et al.* 2015; Lombardozzi *et al.* 2017; Hoshika *et al.* 2018).

Why would plants not completely close their stomata at night? The primary non-adaptive hypothesis that has been proposed is the “leaky stomata” hypothesis, where fully closing stomata could have an energetic cost that plants only pay during very dry conditions and thus stomata remain partially open at night. This hypothesis appears to be at odds with the significant documentation of g_{sn} in dry environments, where the costs of water loss should be high.

The primary adaptive hypotheses that have been proposed center on plant functional response to environmental conditions including water stress, nutrient availability, and oxygen availability. There have been a number of studies suggested that some species can actively reduce or close stomata during the night in response to water stress and/or ABA (Caird *et al.* 2007; Cirelli *et al.* 2015), although several shrub species in North American deserts exhibited differential daytime and nighttime stomatal behavior in response to environmental conditions (Ogle *et al.*, 2012; Zeppel *et al.*, 2012). This could lead to refilling capacitance and removing embolism in stems (Zeppel *et al.* 2014), which would lead to improved early morning photosynthesis (Caird *et al.* 2007). However, experiments manipulating water/ nutrient conditions or vapor pressure deficit (VPD), which can also affect photosynthesis, showed a divergent response of g_{sn} (Caird *et al.* 2007; Zeppel *et al.* 2014).

Studies have also proposed that g_{sn} could benefit plants through increasing nutrient availability for root uptake (Scholz *et al.*, 2007) and oxygen delivery for sapwood parenchyma cells (Daley & Phillips, 2006). The hypothesis of improved nutrient availability has been extensively studied (Caird *et al.*, 2007; Zeppel *et al.*, 2014). Both g_{sn} and E_n result in increased access by roots surfaces to soil nutrients through mass flow and diffusion (Oliveira *et al.* 2010; Kupper *et al.* 2012) and thus likely improves nutrient availability to plants. The causality between g_{sn} and nutrient uptake, however, has garnered weak-to-mixed evidence (Howard & Donovan, 2007; Christman *et al.* 2009; Kupper *et al.* 2012).

An additional adaptive ecological mechanism that has been proposed suggests that g_{sn} could be a strategy to reduce hydraulic redistribution in the soil, thereby keeping water resources close to an individual plant rather than moving that water towards neighboring competitors (Huang *et al.* 2017); this hypothesis has shown some initial empirical support (Neumann *et al.* 2014; Yu *et al.* 2018). Ultimately, the factors or mechanisms affecting g_{sn} remain rather unclear and studies on this hypothesis to date have been largely carried out in a controlled (e.g. greenhouse or growth chamber) environment (Caird *et al.* 2007; Zeppel *et al.* 2014).

Some studies have indicated that there may be genetic controls on g_{sn} (Caird *et al.* 2007; Costa *et al.* 2015; Reuning *et al.* 2015) and that g_{sn} may have a biogeographic signal (Caird *et al.* 2007; Zeppel *et al.* 2014). However, it remains unclear whether or not there is a strong phylogenetic signal in functional traits of g_{sn} (i.e., the tendency for trait relatedness among related species) and whether or not g_{sn} has evolved as an adaptation to climate or soil nutrient conditions in a species' native range. A strong phylogenetic or biogeographic signal could inform the estimates of g_{sn} at large scales (Moles *et al.*, 2005; Swenson *et al.*, 2017), which are currently limited by technical obstacles (De Dios *et al.* 2015) but crucial for Earth system models (Lombardozzi *et al.* 2017). The genetic controls on g_{sn} could also offer new horizons for breeding programs to cultivate crops that have lower g_{sn} and the same growth, thus increasing water-use efficiency (Costa *et al.* 2015; Coupel-Ledru *et al.* 2016). The studies to date only leveraged a narrow spatial range of native habitats with a small number of co-occurring species to examine g_{sn} in native climate conditions (Snyder *et al.* 2003; Ogle *et al.* 2012). While Lombardozzi *et al.* (2017) compiled a large dataset ($n=204$) to better represent g_{sn} in land surface models and allow the comparison of g_{sn} among different functional groups, these observed g_{sn} values were estimated by a variety of methods and measurement conditions, which limits rigorous comparison across functional groups, and had very limited information on boreal climate zones. Hoshika *et al.* (2018) compiled a large dataset to show the correlation between daytime maximum g_s in woody plants and mean annual precipitation, but the information of climatic (biogeographic) controls on g_{sn} is limited.

Thus, there is a critical need for a large common garden study in which the g_{sn} of species from a broad diversity of clades can be sampled in the same climate/growth environment to provide rigorous quantification of cross-species patterns and insights into potential adaptive drivers of g_{sn} . Here, we quantify g_{sn} on 73 species among a number of different clades growing in a common garden in a dry climate (e.g. substantial VPD) to examine the phylogenetic and biogeographic controls on g_{sn} . The species represent various life forms (i.e., trees, shrubs, grasses and forbs) originating from diverse climate zones (i.e., boreal, $n = 32$; temperate dry, $n = 15$; and temperate wet climate, $n = 26$). We ask: (1) is there evidence for a phylogenetic signal in g_{sn} ? (2) does g_{sn} vary among species as a function of their native climate, and soil nutrient conditions and, if so, to which climate or soil nutrient variables? (3) are there consistent differences in g_{sn} among different life forms and climate zones? (4) does g_{sn} correlate with leaf anatomy and physiology among species?

MATERIAL AND METHODS

Study site, species identification, and methods of observations

We carried out this study in the Red Butte Garden in Salt Lake City, Utah, USA (40.7655° N, 111.8238° W), the largest botanical garden in the Intermountain West. The climate is characterized by a semi-desert steppe with hot, dry summers and long, cold winters. Mean annual precipitation is about 400-500 mm with most precipitation occurring in winter and spring. At the beginning of May 2017, we identified 93 species representative of various life forms (i.e., trees, shrubs, grasses, and forbs) (Engemann *et al.*, 2016), leaf forms, and leaf shapes. Species names were confirmed with the Taxonomic Name Resolution Service (TNRS; Boyle *et al.* 2013). Three individuals with similar size and proximity in distance were identified in each species. In each individual, one recently mature and fully-expanded leaf was marked for the measurements of gas exchange and traits. To control for differences in microclimate, leaves on woody plants were located at similar canopy heights and were generally sun-exposed and south-facing.

Nighttime gas exchange was measured for each individual using a LI-6800 (Li-Cor, Inc., Lincoln, NE, USA) with the 6 cm² leaf chamber (circle; radius = 1.38 cm) in a closed system mode. These measurements were conducted on several continuous clear nights (4-5) to ensure similar climate for each sampling event. Sampling was carried out once a month from May to August. For all of the analyses in this study, we used the measurements from one sampling event during June because it best captured the g_{sn} max of all species. Volumetric soil water content at soil depth of 20 cm was measured ($n = 3$ for each species) at locations near to (<1 m from plant base) where gas exchange measurements were made; the measurements were conducted in the late afternoon before nighttime gas exchange using decagon GS3 soil moisture sensor. A circadian rhythm in g_{sn} has been observed in some species (Caird *et al.* 2007; Ogle *et al.* 2012; Resco de Diosa & Gessler, 2018), with a gradual

increase of g_{sn} after midnight and maximum values during predawn hours. Thus, to approximately estimate the maximum g_{sn} across a large sample size of species, nighttime gas exchange measurements were made 2-3 h before dawn. We present the maximum g_{sn} observed, the magnitude of which is quite low relative to daytime g_s , but provides a useful species-level trait similar to daytime maximum stomatal conductance (e.g. Oren et al. 1999). We took the maximum g_{sn} for each of the individuals of a species and then averaged. Thus, the mean of maximum g_{sn} over individuals across species was used for analyses. This allowed for less uncertainty in measurements of g_{sn} over a large sample size of species. During the measurements, reference CO_2 was set to $400 \mu mol mol^{-1}$, while VPD and temperature tracked ambient. To reduce the bias of data recording (logging), the same standard of judging the stability of gas exchange data was used. We monitored the g_{sn} and took the measurement when the slope of g_{sn} vs. time was smaller than $0.0015 mol m^{-2} s^{-2}$. For some species with small or (semi)cylinder shaped leaves that do not completely cover the leaf chamber area, the net gas exchange rate (stomatal conductance and respiration) was determined as $G = G_r \times 6/S$, where G_r is the recorded value of the net gas exchange rate by LI-6800 and S is the surface area (cm^2) of the leaf (Table S1).

Day time gas exchanges were also measured between 09:30 h and 12:00 h on the days before nighttime measurements; the 'one-point method' was then used to estimate maximum carboxylation capacity (V_{cmax}) for each species (De Kauwe *et al.*, 2016). This method requires estimating leaf respiration during the day. Assuming that leaf respiration during the day is 1.5% of V_{cmax} , this method was found to estimate V_{cmax} with an r^2 of 0.95, as compared to the traditional A–Ci curve fitting (De Kauwe *et al.*, 2016). In the middle of June, a subset ($n = 20$) of species across the range of g_{sn} and life forms ($n = 8$ for trees; $n = 3$ for shrubs; $n = 4$ for grasses; $n = 5$ for forbs) were selected for estimates of stomatal density. Stomata peels from adaxial surfaces of the leaves used for gas exchange were sampled using clear nail polish and tape. Stomatal density was counted independently by two trained observers using light microscope images ($n = 10$ per leaf) on each individual leaf peel. At the end of June 2017, a subset ($n = 54$) of species across the range of g_{sn} and life forms were also sampled for estimating specific leaf area (SLA).

Phylogenetic tree, species native ranges and climate

The phylogenetic tree was constructed using *phylomatic* in PHYLOCOM 4.2 (Webb *et al.* 2008) with the 'R20100701' megatree. Approximate crown ages for each clade were calculated using *bladj*. Internal node constraints were from Bell *et al.* (2010) and subsequently corrected for file transcription errors (Gastauer & Meira-Neto, 2013). To construct a binary tree, we used the *multi2di* function in the 'ape' package.

Global Biodiversity Information Facility (GBIF; <http://www.gbif.org>) was used to determine native distribution of the species in May 2018. To extract species' geo-referenced locations (latitude and longitude), we first used the 'dismo' R package. We then used the following criteria (Zohner *et*

al., 2016) to filter reliable records (locations) of species: 1) only records from a species' native continent (North America, Europe, and Asia) were included; 2) coordinate duplicates within a species were removed; 3) records based on fossil specimen were removed; 4) spatially clustered records within 10 km were removed to correspond with the spatial resolution (bio 2.5m; 10 km) of WorldClim (<http://www.worldclim.org/bioclimate>) used to determine the climate of native species ranges; 5) hybrid species and species without records in GBIF were excluded. This led to a total sample size of 73 species with adequate distribution data to calculate climate-of-origin (Table S1).

Species-specific climate ranges were derived from WorldClim variables based on species' georeferenced locations. WorldClim variables included annual mean temperature (BIO1), mean temperature of driest quarter (BIO9), mean temperature of warmest quarter (BIO10), annual precipitation (BIO12), precipitation of driest quarter (BIO17), precipitation of warmest quarter (BIO18), annual mean vapor pressure deficit (VPD), vapor pressure deficit of driest quarter (VDQ), and vapor pressure deficit of warmest quarter (VWQ) and were chosen based on previous research on g_{sn} (Daley & Phillips, 2006; Caird *et al.* 2007; Dawson *et al.* 2007; Zeppel *et al.* 2014). Temperature and precipitation variables were downloaded from the standard WorldClim Bioclimatic variables for WorldClim v2 (<http://worldclim.org/version2>), while VPD, VDQ, VWQ were not available as WorldClim outputs. Thus, we quantified VPD, VDQ, VWQ following the same protocol as the outputs of standard WorldClim Bioclimatic variables (<http://worldclim.org/bioclimate>). With respect to the impacts of soil nutrients, we used a global soil nitrogen (SN) database with > 3500 soil profiles (Zinke *et al.* 1998) and inverse distance interpolation approach to generate a global raster of soil nitrogen. We also used a global raster of soil organic carbon (SOC) at 2 m soil depth with 10 km spatial resolution, which plays an important role in nutrient cycling (Schmidt *et al.* 2011) and thus was represented here as a coarse proxy for soil nutrients; the data was downloaded from <https://www.soilgrids.org>.

To investigate the difference of g_{sn} among climate zones, the species' georeferenced locations were assigned to sub-climate zones using the Koeppen–Geiger system (Peel *et al.*, 2007). When species were located in multiple sub-climate zones, the sub-climate zone where the species has the maximum number of records was used (Table S1). To evaluate the g_{sn} on a larger (climate zone) scale, we then joined sub-climate zones into broader climate zones - temperate dry (TeD), temperate wet (TeW), and boreal (Bo) climate zones, following the criteria: TeD (BSk, n = 10; Csa, n = 4; Csb, n = 1); TeW (Cwa, n = 1; Cfa, n = 14; Cfb, n = 11); Bo (Dwb, n = 1; Dfa, n = 4; Dfb, n = 26; Dfc, n = 1) (Peel *et al.* 2007).

Data analysis

Two complementary approaches were used to determine how species' phylogenetic relationships and native climate and soil nutrient ranges (biogeography) affects g_{sn} .

The first approach was to determine the phylogenetic and biogeographic signals of g_{sn} separately. To this end, we tested for phylogenetic signal in mean g_{sn} among the three individuals in each species using Pagel's lambda (λ) following Münkemüller *et al.* (2012). Values of λ approaching 1 indicate the fit of a Brownian motion model of evolution and suggest that mean values of g_{sn} are more closely related among relatives than expected by chance, while values approaching 0 indicate phylogenetic independence. Pagel's lambda (λ) was determined using the *phylosig* function in the 'phytools' package; 1000 simulations of Pagel's lambda (λ) were performed and the significance was assessed using a likelihood ratio test (Revell 2012).

For the biogeographic signal of g_{sn} , we determined the biogeographic signal of g_{sn} by testing which species' native climate and soil nutrient variables (BIO1, BIO9, BIO10, BIO12, BIO17, BIO18, VPD, VDQ, VWQ, SN, SOC) were important in affecting g_{sn} using multivariate linear regression. To avoid multicollinearity in our models, we used a pairwise correlation matrix and removed any variable that had high correlations ($R > 0.7$) with other predictor variables following previous studies (Anderegg *et al.* 2013). The variables (BIO1, BIO10, BIO12, BIO17, VDQ, SOC) that gave the best prediction of species-level variation in g_{sn} were retained in the model. SOC was used as the sole soil nutrient variable because SOC and SN were highly correlated.

After standardizing all independent and dependent variables to z-scores, we then used two methods of investigating variable importance of this reduced set of predictor variables in affecting g_{sn} . In the first approach, both forward and backward stepwise model selection via Akaike Information Criterion were used to determine the most parsimonious model and the coefficients of the predictor variables that remained in the model (Burnham & Anderson, 2004). In the second approach, machine learning algorithm Random Forests were used to determine variable importance for each variable (Breiman, 2001). Higher values of the mean decrease in accuracy (%IncMSE) indicate the increased importance of the variables. We ran 1000 simulations of machine learning algorithm Random Forest and calculated mean \pm standard deviation values of %IncMSE.

In the second approach, we used hierarchical Bayesian models to investigate the influence of native climate and soil nutrient ranges (biogeography) on g_{sn} by accounting for possible effects of shared evolutionary history (phylogenetics). To this end, using the Bayesian phylogenetic regression method (Villemereuil *et al.*, 2012), we incorporated the phylogenetic structure of the data into the hierarchical Bayesian models by converting the 73-species ultrametric phylogeny into a scaled (0–1) variance–covariance matrix (Zohner *et al.* 2016). The resulting posterior distributions are a direct statement of the effect magnitude of species native climate and soil nutrient (represented by mean and median values of climate and soil nutrient ranges) on mean g_{sn} .

Using the hierarchical Bayesian models accounting for possible effects of shared evolutionary history, we also separately investigated the difference of g_{sn} among different life forms (trees, shrubs, grasses, and forbs) and among different climate zones (Bo, TeD, and TeW). In these analyses, different life forms (trees, shrubs, grasses, and forbs) or different climate zones were treated as binary (independent) variables. We also incorporated plant functional types (trees, shrubs, grasses, and forbs) as random effects into the hierarchical Bayesian models because g_{sn} was significantly different among life forms and then examined the influence of native climate and soil nutrient ranges (biogeography) on g_{sn} . To investigate the sensitivity of results to number of observations (records) in each species in GBIF, we excluded species with less than 30 geo-referenced records within their native continent. Most of the species with limited observations were from Asia (Table S1). All of the analysis using hierarchical Bayesian models used standardised data and the results can be interpreted as relative effect sizes. Thus, to better visualize the variations of unstandardized g_{sn} among different life forms and climate zones, we 1) used box and whisker plots to display the distribution of g_{sn} and 2) analyzed/plotted the mean and 95% confidence interval.

Finally, we used univariate linear regression analysis to examine the relationships between g_{sn} and a number of environmental, physiological and morphological variables including volumetric soil water content, day time g_s , photosynthetic rates, maximum carboxylation capacity of photosynthesis (V_{cmax}), nighttime respiration, stomatal density, and specific leaf area (SLA). In addition, due to the strong relationship between V_{cmax} and g_{sn} , we included V_{cmax} as a fixed effect factor and plant functional group as a random effect factor in the hierarchical Bayesian models to investigate the influence of biogeographic climate on g_{sn} .

Data availability

The data supporting the results are archived on the Hive, the University of Utah's Open Access Institutional Data Repository and the data DOI is <https://doi:10.7278/S50D-E9J1-NYG0>.

RESULTS

We observed a wide range of g_{sn} across the diverse set of species, with mean g_{sn} ranging from 0.002 mol m⁻² s⁻¹ to 0.05 mol m⁻² s⁻¹ across species and generally smaller values in conifers (Fig. 1). Pagel's lambda (λ) in our species was 0.37 (n = 73) and the p-value of the likelihood ratio test was 0.047. This indicates weak evidence that mean g_{sn} is more closely related among relatives than would be expected by chance alone under a model of Brownian motion.

With respect to the influence of biogeography examined via model selection, we found that mean annual precipitation (MAP) of species' native climate ranges was the single best predictor of g_{sn} ($P = 0.008$ for mean and $P = 0.007$ for median) and plants from locations with lower precipitation had higher g_{sn} (Figs 2a, S1a). Precipitation of the driest quarter (PDQ) was retained in the model selection, but its relationships with g_{sn} were not significant ($P = 0.122$ for mean and $P = 0.086$ for median). In contrast, both soil nitrogen (SN) and soil organic carbon (SOC), used as a coarse proxy for soil nutrients, were not good predictors of g_{sn} and were not retained in the model. We observed similar patterns using the machine learning algorithm Random Forests, which showed highest values of the mean decrease in accuracy (%IncMSE) and thus the importance of MAP in native climate in influencing mean g_{sn} (Figs 2b, S1b).

Using hierarchical Bayesian models to investigate the influence of biogeographic control on g_{sn} , while accounting for possible effects of shared evolutionary history, we found that Pagel's λ values were significantly greater than 0.2 for the scenarios of using mean and median values of native climate and soil nutrient condition ranges (AMT, MTW, MAP, PDQ, VDQ, SOC or SN), respectively (Figs. 3a, S2). Similar to the results above, this provides some evidence for g_{sn} values being more closely related among relatives than would be expected by chance alone. After accounting for the plant phylogenetic differences, MAP still showed the significant and negative relationship with g_{sn} ($n = 73$) both using mean and median values of native climate and soil nutrient condition ranges (Figs. 3b, c, S2). This pattern was robust after excluding species ($n = 9$) with less than 30 georeferenced records in GBIF (Table S1; Fig. S3).

The results, without accounting for possible effects of shared evolutionary history, demonstrated a higher g_{sn} in herbaceous species (grasses and herbs) than trees and/or shrubs (Figs 4a, S4a) and a higher g_{sn} in boreal climate zone than temperate climate zones (Figs 4b, S4b). Using the hierarchical Bayesian models to account for possible effects of shared evolutionary history, the results demonstrated similar patterns of higher g_{sn} in herbaceous species and in the boreal climate zone (Fig. 4c, d), but the differences in g_{sn} across species between the boreal and temperate climate zones were large (Figs 4d, S4b). Since g_{sn} largely varied across life forms, we accounted for the influence of life forms by incorporating them as random (binary) factors into the hierarchical Bayesian models to examine the biogeographic control on g_{sn} . The results still showed the significant negative relationship between g_{sn} ($n = 73$) and MAP, in contrast to PDQ and SOC (Fig. S5).

The univariate regression analysis showed a non-significant correlation between g_{sn} and the local soil water conditions in the common garden ($P = 0.35$, Fig. S6a), suggesting minimal influence of local soil conditions on g_{sn} . The g_{sn} was significantly related to day time stomatal conductance ($P < 0.0001$, Fig. S6b), photosynthetic rate ($P < 0.0001$, Fig. S6c) and higher night

respiration ($P < 0.0001$, Fig. S6d) across species. The results also showed that g_{sn} significantly increased with maximum carboxylation capacity (V_{cmax} ; $n = 73$) ($P = 0.0006$, Fig. S7a), while the relationships with stomatal density ($n = 20$; $P = 0.17$) (Fig. S7b) and specific leaf area (SLA) ($n = 54$; $P = 0.98$) (Fig. S7c) were not significant. Finally, to account for the effects of V_{cmax} in biogeographic signals, we also incorporated it as a fixed effect factor plus plant functional group as a random effect factor into the hierarchical Bayesian models. Accounting for these effects did not change the results (Fig. S8). Overall, the analyses robustly suggested that MAP was the best predictor of g_{sn} ; plants in locations with lower rainfall conditions had higher g_{sn} .

DISCUSSION

We analyzed the underlying phylogenetic and biogeographic influences, as well as leaf morphological and physiological traits, on plant nighttime stomatal conductance by measuring a suite of diverse species grown in a common climate. The values of g_{sn} were within the lower ranges of previously reported values (Caird *et al.* 2007; Zeppel *et al.* 2014; Lombardozzi *et al.* 2017). We found weak evidence for a phylogenetic pattern of g_{sn} wherein closely related species had more similar g_{sn} than expected by chance (Figs 1 and 3). For instance, the conifers (e.g., Pinales) all had similarly low mean g_{sn} , while the grasses (e.g., Poaceae) all had particularly high mean g_{sn} . This suggests that estimates of g_{sn} at large scales carried out by reconstructing g_{sn} based on their phylogenetic positions may not be an appropriate approach (Moles *et al.* 2005; Swenson *et al.* 2017). We did, however, detect substantial differences in g_{sn} between life forms of grasses versus woody plants, which could be valuable for quantifying and simulating the large-scale impacts of g_{sn} on carbon/water cycling in Earth system models that typically simulate ecosystems with “plant functional types” (Lombardozzi *et al.* 2017).

Mean annual precipitation (MAP) rather than temperature has been found to affect daytime maximum g_s (Hoshika *et al.*, 2018). In this study, we found robust evidence of g_{sn} adaptations to species’ native climate range instead of local soil (water) conditions. Even after accounting for weak patterns of phylogenetic conservatism, species typically found in locations with lower MAP had higher g_{sn} (Fig. 3). This pattern does not change based on choice of number of species (Fig. S3), the incorporation of plant functional group as a random effect (Fig. S5), or V_{cmax} as a fixed effect (Fig. S8). Our results are consistent with previous studies that found higher E_n (20-30%) relative to daytime rates among species in deserts and savannas (Bucci *et al.* 2004; Caird *et al.* 2007; Ogle *et al.*, 2012). These results are interesting because they suggest that in dry regions where water is frequently limiting plant growth (Yu *et al.* 2016; Chen *et al.* 2018), plants exhibit substantial nighttime stomatal conductance. This supports an adaptive benefit of nighttime stomatal conductance because the fitness costs of water loss in these regions are likely high. In other words, the non-adaptive “leaky stomata”

hypothesis would predict that highest g_{sn} should occur in regions where the fitness cost of water loss during the night is lowest (i.e. wet regions), which is not what we observed.

Previous studies have extensively investigated the impacts of soil nutrients on g_{sn} and have shown divergent response of g_{sn} to soil nutrient conditions (Howard & Donovan, 2007; Christman *et al.* 2009; Kupper *et al.* 2012). Our study did not find strong evidence for a correlation between g_{sn} and the native soil nitrogen (SN) or soil organic carbon (SOC) (Figs. 3, S2, S5, S8), at least within the coarse constraints of the global datasets analyzed here. While we did not measure the local soil nutrients in the common garden, it is likely that local soil nutrient conditions would have minimal influence on g_{sn} . In fact, a causal relationship between g_{sn} and soil/plant nutrients still remains highly elusive (Kupper *et al.* 2012). In contrast to the hypothesis and evidence that g_{sn} changes with low soil nutrient conditions (Scholz *et al.* 2007), extensive studies have shown the opposite pattern: higher rates of g_{sn} in species with relatively high overall growth rate and leaf/soil nitrogen concentrations (Daley & Phillips, 2006; Phillips *et al.* 2010; Kupper *et al.* 2012).

Our observation that species from dry regions have higher g_{sn} is consistent with hypotheses that plant night stomatal opening may benefit plants by refilling capacitance and removing embolism in stems (Zeppel *et al.* 2014), especially considering that plants are water stressed and in some cases may have higher risk of embolism in drylands (Tyree & Zimmermann, 2002; Brodersen & McElrone, 2013). Thus, the large variation in g_{sn} in lower mean annual precipitation (i.e., MAP < 1200 mm) (Fig. 2) may reflect differences in plant functional strategies with respect to capacitance and vulnerability to embolism (Brodersen & McElrone, 2013; McCulloch *et al.* 2014; Zeppel *et al.* 2014). Alternatively, we suggest that our biogeographic patterns are more consistent with the hypothesis that nighttime water loss may provide a competitive advantage by curtailing passive water flow or hydraulic redistribution (Neumann *et al.* 2014; Yu *et al.* 2018), thereby improving plant fitness where plants compete belowground for water. Maintaining stomata slightly open would create a water potential gradient in the plant-soil hydraulic continuum that would favor keeping soil water close to an individual plant's rooting system and prevent water from diffusing along passive water potential gradients in the soil to neighboring plants (Huang *et al.* 2017). Plant competition for water is likely most intense in dry regions and these scenarios are exactly where we observed the highest g_{sn} (Figs 2, 3). This hypothesis of hydraulic redistribution may be more important for woody plants, which usually have deep roots and thus higher rates of hydraulic redistribution than herbaceous species (Neumann & Cardon, 2012; Yu & D'Odorico, 2015).

We observed the shifted and higher rates of g_{sn} in forbs than grasses after accounting for plant phylogenetics, thus suggesting the role of plant phylogenetics in affecting g_{sn} across life forms (Figs 4a, S4). However, regardless of influence of plant phylogenetics, higher rates of g_{sn} were found in herbaceous species (grasses and forbs) than woody species (Figs 4a, S4), similar to other studies

(Lombardozi *et al.* 2017; O’Keefe & Nippert, 2018). The high rate of g_{sn} in herbaceous species may result from relatively high overall growth rate (Chen *et al.* 2018) and thus plant photosynthesis and starch accumulation, which have been found to affect guard cell osmoregulation and increase g_{sn} (Lascève *et al.* 1997; Easlon & Richards, 2009), consistent with our observed positive relationship between daytime stomatal conductance and photosynthesis and g_{sn} (Fig. S6). The high rate of g_{sn} in herbaceous species may support the hypothesis of the competitive advantage of soil moisture uptake by herbaceous species in shallow soil due to the high density or surface areas of fine roots (Steudle, 2000; Lombardozi *et al.* 2017; O’Keefe & Nippert, 2018). In drylands, precipitation events more often wet soil shallow layers (Yu *et al.* 2016; Chen *et al.* 2018) and it could be advantageous for herbaceous species to preferentially use the shallow soil moisture through daytime and nighttime water uptake/transpiration. This reduces the diffusion of water along passive water potential gradients in the soil to its competitors (i.e., woody plants) and can even lead to the bottleneck effect of restricting the tree recruitment (Bond 2008).

Previous studies have found high values of g_{sn} in tropical deciduous trees (Caird *et al.* 2007), as well as high values of E_n estimated by sap flow in Mediterranean ecosystems (Barbeta *et al.*, 2012) and tropical rainforests (Wallace & McJannet, 2010). All of these studies, however, were limited to a few species and lacking information from boreal climate zone. This study found higher g_{sn} in species from boreal as compared to temperate climate zones regardless of plant phylogenetics (Fig. 4b, d). After accounting for plant phylogenetics, the higher g_{sn} in the boreal climate zone was even more striking (Figs 4d, S4b), in which the conifers dominate and had similarly low g_{sn} . However, we note that our species mainly capture the drier regions of boreal climate zone (Fig. S9), which have likely led to the high observed g_{sn} , consistent with the effects of MAP on g_{sn} . The substantial role of climate-of-origin in influencing cross-species patterns of nighttime stomatal conductance sheds light on potential adaptive drivers of nighttime water loss. Thus, more studies evaluating g_{sn} and its role of native climate ranges are greatly needed in a diversity of vegetation types and across climates.

Our findings that species g_{sn} are coupled to, and thus potentially adaptations to, native climate indicates that reducing g_{sn} through breeding or genetic modifications may impair plant growth. This was demonstrated by an earlier study in *Arabidopsis thaliana* mutant (Christman *et al.* 2008). However, two recent studies on mutants of *Arabidopsis thaliana* and *Vitis vinifera* found that growth was unaffected by manipulated reductions in g_{sn} and transpiration (Costa *et al.* 2015; Coupel-Ledru *et al.* 2016). The divergent results of these studies may be due to different environmental conditions (i.e., water availability) during experimental treatments. In fact, growth was not affected by reduced g_{sn} or E_n on *Arabidopsis* only in well-water conditions where the fitness cost of water loss is low (Christman *et al.* 2009).

Our study has multiple implications for evaluating current ecosystem carbon and water fluxes and their dynamics under future climate change scenarios. First, our finding of higher g_{sn} rates in plants from dry regions (Fig. 2) (Bucci *et al.* 2004; Caird *et al.* 2007; Ogle *et al.* 2012) highlights the need to incorporate representations of g_{sn} in estimating ecosystem carbon/water fluxes, particularly in drylands (Dios *et al.* 2015; Lombardozzi *et al.* 2017). Second, in increasingly changing climate (Easterling 2000), nighttime water loss is likely to alter future ecosystem carbon/water fluxes, while quantification of its impacts remains challenging because of uncertainty of the precipitation projections (Woldemeskel *et al.* 2015). Thus, critical consideration of the phylogenetic and biogeographic patterns of g_{sn} can help shed insight into the adaptive benefits of g_{sn} in plants and inform modeling efforts to predict ecosystem carbon/water dynamics under climate change scenarios. Third, high values of g_{sn} correspond with higher values of V_{cmax} , which typically leads to higher plant night respiration. This further suggests the higher fitness cost of water loss in dry regions, whereby the higher g_{sn} should confer a functional advantage.

Acknowledgements

WRLA acknowledges funding from the David and Lucille Packard Foundation, the University of Utah Global Change and Sustainability Center, NSF Grants 1714972 and 1802880, and the USDA National Institute of Food and Agriculture, Agricultural and Food Research Initiative Competitive Programme, Ecosystem Services and Agro-ecosystem Management, grant no. 2018-67019-27850. We would like to thank Rosanise Odell, Mary Beninati, Jaycee Cappaert and Michaela Lemen for the help in the experiments.

Author contributions

KY and WRLA designed the study with inputs from GRG; KY, YW and WRLA collected the data; KY performed data analysis with inputs from GRG; KY wrote the manuscript with revisions from all coauthors.

REFERENCES

- Anderegg LDL, Anderegg WRL, Abatzoglou J, Hausladen AM, Berry JA. 2013.** Drought characteristics' role in widespread aspen forest mortality across Colorado, USA. *Global Change Biology* **19**: 1526–1537.
- Anderegg WRL, Wolf A, Arango-Velez A, Choat B, Chmura DJ, Jansen S, Kolb T, Li S, Meinzer FC, Pita P, *et al.* 2018.** Woody plants optimise stomatal behaviour relative to hydraulic risk. *Ecology Letters*. **21**: 968-967.

Barbeta A, Ogaya R, Peñuelas J. 2012. Comparative study of diurnal and nocturnal sap flow of *Quercus ilex* and *Phillyrea latifolia* in a Mediterranean holm oak forest in Prades (Catalonia, NE Spain). *Trees - Structure and Function*. **26**: 1651-1659.

Bell CD, Soltis DE, Soltis PS. 2010. The age and diversification of the angiosperms re-revisited. *American Journal of Botany* **97**: 1296–1303.

Berry JA, Beerling DJ, Franks PJ. 2010. Stomata: Key players in the earth system, past and present. *Current Opinion in Plant Biology*. **13**: 232-239.

Bond WJ. 2008. What Limits Trees in C₄ Grasslands and Savannas? *Annual Review of Ecology, Evolution, and Systematics* **39**: 641–659.

Boyle B, Hopkins N, Lu Z, Raygoza Garay JA, Mozzherin D, Rees T, Matasci N, Narro ML, Piel WH, McKay SJ, et al. 2013. The taxonomic name resolution service: An online tool for automated standardization of plant names. *BMC Bioinformatics* **14**: 16.

Breiman L. 2001. Random forests. *Machine Learning* **45**: 5–32.

Brodersen CR, McElrone AJ. 2013. Maintenance of xylem Network Transport Capacity: A Review of Embolism Repair in Vascular Plants. *Frontiers in Plant Science*. 104, 108

Brodrribb TJ, McAdam SAM. 2017. Evolution of the Stomatal Regulation of Plant Water Content. *Plant Physiology*. **174**: 639-649.

Bucci SJ, Scholz FG, Goldstein G, Meinzer FC, Hinojosa JA, Hoffmann WA, Franco AC. 2004. Processes preventing nocturnal equilibration between leaf and soil water potential in tropical savanna woody species. *Tree Physiology*. **24**: 1119-1127.

Buckley TN. 2005. The control of stomata by water balance. *New Phytologist*. **168**: 275-292.

Burnham KP, Anderson DR. 2004. Multimodel inference: Understanding AIC and BIC in model selection. *Sociological Methods and Research* **33**: 261–304.

Caird MA, Richards JH, Donovan LA. 2006. Nighttime stomatal conductance and transpiration in C₃ and C₄ Plants. *Plant Physiology*. **143**: 4-10.

Chen N, Jayaprakash C, Yu K, Guttal V. 2018. Rising variability, not slowing down, as a leading indicator of a stochastically driven abrupt transition in a dryland ecosystem. *The American Naturalist*. **191**: E1-E14.

Christman MA, Donovan LA, Richards JH. 2009. Magnitude of nighttime transpiration does not affect plant growth or nutrition in well-watered *Arabidopsis*. *Physiologia Plantarum*. **136**: 264-273.

This article is protected by copyright. All rights reserved.

Christman MA, Richards JH, McKay JK, Stahl E a, Juenger TE, Donovan L a. 2008. Genetic variation in *Arabidopsis thaliana* for night-time leaf conductance. *Plant, cell & environment*. **31**: 1170-1178.

Cirelli D, Equiza MA, Lieffers VJ, Tyree MT. 2015. *Populus* species from diverse habitats maintain high night-time conductance under drought. *Tree Physiology*. **36**: 229-242.

Costa JM, Monnet F, Jannaud D, Leonhardt N, Ksas B, Reiter IM, Pantin F, Genty B. 2015. OPEN ALL NIGHT LONG: The Dark Side of Stomatal Control 1. *Plant Physiology*. **167**: 289-294.

Coupel-Ledru A, Lebon E, Christophe A, Gallo A, Gago P, Pantin F, Doligez A, Simonneau T. 2016. Reduced nighttime transpiration is a relevant breeding target for high water-use efficiency in grapevine. *Proceedings of the National Academy of Sciences*. **113**: 8963-8968.

Daley MJ, Phillips NG. 2006. Interspecific variation in nighttime transpiration and stomatal conductance in a mixed New England deciduous forest. *Tree Physiology*. **26**: 411-419.

Dawson TE, Burgess SSO, Tu KP, Oliveira RS, Santiago LS, Fisher JB, Simonin KA, Ambrose AR. 2007. Nighttime transpiration in woody plants from contrasting ecosystems. *Tree Physiology*. **27**, 561–575.

De Dios VR, Roy J, Ferrio JP, Alday JG, Landais D, Milcu A, Gessler A. 2015. Processes driving nocturnal transpiration and implications for estimating land evapotranspiration. *Scientific Reports*. **5**:10975.

Easterling DR. 2000. Climate Extremes: Observations, Modeling, and Impacts. *Science*. **289**: 2068-2074.

Easlon HM, Richards JH. 2009. Photosynthesis affects following night leaf conductance in *Vicia faba*. *Plant, Cell and Environment* **32**: 58–63.

Engemann K, Sandel B, Boyle BL, Enquist BJ, Jørgensen PM, Kattge J, McGill BJ, Morueta-Holme N, Peet RK, Spencer NJ, et al. 2016. A plant growth form dataset for the New World. *Ecology* **97**: 3243.

Franks PJ, Berry JA, Lombardozzi DL, Bonan GB. 2017. Stomatal Function across Temporal and Spatial Scales: Deep-Time Trends, Land-Atmosphere Coupling and Global Models. *Plant Physiology*. **174**: 583-602.

Gastauer M, Meira-Neto JAA. 2013. Avoiding inaccuracies in tree calibration and phylogenetic community analysis using Phylocom 4.2. *Ecological Informatics* **15**: 85–90.

Hoshika Y, Osada Y, de Marco A, Peñuelas J, Paoletti E. 2018. Global diurnal and nocturnal parameters of stomatal conductance in woody plants and major crops. *Global Ecology and Biogeography* 27: 257–275.

Howard AR, Donovan LA. 2006. Helianthus Nighttime Conductance and Transpiration Respond to Soil Water But Not Nutrient Availability. *PLANT PHYSIOLOGY* 143: 145–155.

Huang C-W, Domec J-C, Ward EJ, Duman T, Manoli G, Parolari AJ, Katul GG. 2017. The effect of plant water storage on water fluxes within the coupled soil-plant system. *New Phytologist* 213: 1093–1106.

Jasechko S, Sharp ZD, Gibson JJ, Birks SJ, Yi Y, Fawcett PJ. 2013. Terrestrial water fluxes dominated by transpiration. *Nature*. 496: 347–350.

Lascève G, Leymarie J, Vavasseur A. 1997. Alterations in light-induced stomatal opening in a starch-deficient mutant of *Arabidopsis thaliana* L. deficient in chloroplast phosphoglucomutase activity. *Plant, Cell and Environment* 20: 350–358.

Münkemüller T, Lavergne S, Bzeznik B, Dray S, Jombart T, Schiffers K, Thuiller W. 2012. How to measure and test phylogenetic signal. *Methods in Ecology and Evolution* 3: 743–756.

Neumann RB, Cardon ZG. 2012. The magnitude of hydraulic redistribution by plant roots: A review and synthesis of empirical and modeling studies. *New Phytologist* 194: 337–352.

Neumann RB, Cardon ZG, Teshera-Levy J, Rockwell FE, Zwieniecki MA, Holbrook NM. 2014. Modelled hydraulic redistribution by sunflower (*Helianthus annuus* L.) matches observed data only after including night-time transpiration. *Plant, Cell and Environment* 37: 899–910.

Novick KA, Oren R, Stoy PC, Siqueira MBS, Katul GG. 2009. Nocturnal evapotranspiration in eddy-covariance records from three co-located ecosystems in the Southeastern U.S.: Implications for annual fluxes. *Agricultural and Forest Meteorology* 149: 1491–1504.

De Kauwe MG, Lin YS, Wright IJ, Medlyn BE, Crous KY, Ellsworth DS, Maire V, Prentice IC, Atkin OK, Rogers A, *et al.* 2016. A test of the ‘one-point method’ for estimating maximum carboxylation capacity from field-measured, light-saturated photosynthesis. *New Phytologist* 210: 1130–1144.

Kupper P, Rohula G, Saksing L, Sellin A, Löhmus K, Ostonen I, Helmisaari HS, Söber A. 2012. Does soil nutrient availability influence night-time water flux of aspen saplings? *Environmental and Experimental Botany* 82: 37–42.

Lombardozi DL, Zeppel MJB, Fisher RA, Tawfik A. 2017. Representing nighttime and minimum

conductance in CLM4.5: Global hydrology and carbon sensitivity analysis using observational constraints. *Geoscientific Model Development* **10**: 321–331.

McAdam SAM, Brodribb TJ. 2015. The Evolution of Mechanisms Driving the Stomatal Response to Vapor Pressure Deficit. *Plant Physiology* **167**: 833–843.

Mcculloh KA, Johnson DM, Meinzer FC, Woodruff DR. 2014. The dynamic pipeline: Hydraulic capacitance and xylem hydraulic safety in four tall conifer species. *Plant, Cell and Environment*. **37**: 1171-1183.

Moles AT, Ackerly DD, Webb CO, Tweddle JC, John B, Westoby M, Dickie JB, Westoby M. 2005. A brief history of seed size. *Science*. 5709, 576-580.

Ogle K, Lucas RW, Bentley LP, Cable JM, Barron-Gafford GA, Griffith A, Ignace D, Jenerette GD, Tyler A, Huxman TE, et al. 2012. Differential daytime and night-time stomatal behavior in plants from North American deserts. *New Phytologist*. **194**: 464-476.

O’Keefe K, Nippert JB. 2018. Drivers of nocturnal water flux in a tallgrass prairie. *Functional Ecology* **32**: 1155–1167.

Oliveira EMM, Ruiz HA, Alvarez V VH, Ferreira PA, Costa FO, Almeida ICC. 2010. Nutrient supply by mass flow and diffusion to maize plants in response to soil aggregate size and water potential. *Revista Brasileira de Ciência do Solo* **34**: 317–328.

Peel MC, Finlayson BL, McMahon TA. 2007. Updated world map of the Köppen-Geiger climate classification. *Hydrology and Earth System Sciences* **11**: 1633–1644.

Resco de Dios V, Gessler A. 2018. Circadian regulation of photosynthesis and transpiration from genes to ecosystems. *Environmental and Experimental Botany* **152**: 37–48.

Reuning GA, Bauerle WL, Mullen JL, Mckay JK. 2015. Combining quantitative trait loci analysis with physiological models to predict genotype-specific transpiration rates. *Plant, Cell and Environment*. **38**: 710-717.

Revell LJ. 2012. phytools: An R package for phylogenetic comparative biology (and other things). *Methods in Ecology and Evolution* **3**: 217–223.

Scholz FG, Bucci SJ, Goldstein G, Meinzer FC, Franco AC, Miralles-Wilhelm F. 2007. Removal of nutrient limitations by long-term fertilization decreases nocturnal water loss in savanna trees. In: *Tree Physiology*. **27**: 551-559.

Schmidt MWI, Torn MS, Abiven S, Dittmar T, Guggenberger G, Janssens IA, Kleber M, Kögel-

Knabner I, Lehmann J, Manning DAC, et al. 2011. Persistence of soil organic carbon as an ecosystem property. *Nature* **478**: 49–56.

Snyder KA, Richards JH, Donovan LA. 2003. Night-time conductance in C₃ and C₄ species: Do plants lose water at night? *Journal of Experimental Botany*. **54**: 861-865.

Steudle E. 2000. Water uptake by plant roots: An integration of views. *Plant and Soil*. **226**: 45-56.

Swenson NG, Weiser MD, Mao L, Araújo MB, Diniz-Filho JAF, Kollmann J, Nogués-Bravo D, Normand S, Rodríguez MA, García-Valdés R, et al. 2017. Phylogeny and the prediction of tree functional diversity across novel continental settings. *Global Ecology and Biogeography*. **26**: 553-562.

Tyree MT, and Zimmermann MH. 2002. *Xylem Structure and the Ascent of Sap*. New York: Springer-Verlag.

Villemereuil P De, Wells JA, Edwards RD, Blomberg SP. 2012. Bayesian models for comparative analysis integrating phylogenetic uncertainty. *BMC Evolutionary Biology* **12**: 102.

Wallace J, McJannet D. 2010. Processes controlling transpiration in the rainforests of north Queensland, Australia. *Journal of Hydrology*. **384**: 107-117.

Webb CO, Cannon CH, Davies SJ. 2008. Ecological organization, biogeography, and the phylogenetic structure of tropical forest tree communities. In: *Tropical Forest Community Ecology* (eds Carson, W. & Schnitzer, S.). Singapore: Wiley Blackwell, 79–97.

Yu K, D’Odorico P. 2015. Hydraulic lift as a determinant of tree-grass coexistence on savannas. *New Phytologist* **207**: 1038–1051.

Yu K, Okin GS, Ravi S, D’Odorico P. 2016. Potential of grass invasions in desert shrublands to create novel ecosystem states under variable climate. *Ecohydrology*. **9**: 1496-1506.

Yu T, Feng Q, Si J, Mitchell PJ, Forster MA, Zhang X, Zhao C. 2018. Depressed hydraulic redistribution of roots more by stem refilling than by nocturnal transpiration for *Populus euphratica* Oliv. in situ measurement. *Ecology and Evolution* **8**: 2607–2616.

Zeppel MJB, Lewis JD, Chaszar B, Smith RA, Medlyn BE, Huxman TE, Tissue DT. 2012. Nocturnal stomatal conductance responses to rising CO₂, temperature and drought. *New Phytologist*.

Zeppel MJB, Lewis JD, Phillips NG, Tissue DT. 2014. Consequences of nocturnal water loss: A synthesis of regulating factors and implications for capacitance, embolism and use in models. *Tree Physiology*. **193**: 929-938.

Zinke, P.J., A.G. Stangenberger, W.M. Post, W.R. Emanuel, and J.S. Olson. 1998. Global Organic

This article is protected by copyright. All rights reserved.

Zohner CM, Benito BM, Svenning JC, Renner SS. 2016. Day length unlikely to constrain climate-driven shifts in leaf-out times of northern woody plants. *Nature Climate Change* **6**: 1120–1123.

Supporting Information

Additional supporting information may be found in the online version of this article.

Fig. S1 Relationship between species' maximum plant night time stomatal conductance (g_{sn}) and median of annual precipitation (MAP).

Fig. S2 Relationship between species' maximum plant night time stomatal conductance (g_{sn}) and its native climate and soil nutrients (soil nitrogen, SN) estimated from hierarchical Bayesian models.

Fig. S3 Relationship between species' maximum plant night time stomatal conductance (g_{sn}) and its native climate and soil nutrients (soil organic matter, SOC) estimated from hierarchical Bayesian models after excluding species with less than 30 georeferenced records in GBIF.

Fig. S4 Means and 95% CIs of g_{sn} among different life forms and different climate zones without accounting for possible effects of shared evolutionary history (phylogenetics).

Fig. S5 Relationship between species' maximum plant night time stomatal conductance (g_{sn}) and its native climate and soil nutrients (soil organic matter, SOC) estimated from hierarchical Bayesian models which also account for plant life forms as a random effect.

Fig. S6 Relationship between species' maximum plant night time stomatal conductance (g_{sn}) and local volumetric soil water content estimated by univariate regression analysis.

Fig. S7 Relationship between species' maximum plant night time stomatal conductance (g_{sn}) and day time plant stomatal conductance (g_{sd}), and plant traits.

Fig. S8 Relationship between species' maximum plant night time stomatal conductance (g_{sn}) and its native climate and soil nutrients (soil organic matter, SOC) estimated from hierarchical Bayesian models which also account for plant life forms as a random effect and maximum carboxylation capacity (V_{cmax}) as a fixed effect.

Fig. S9. Annual precipitation (MAP, mean and 95% CIs) in boreal (Bo), temperate dry (TeD), and temperate wet (TeW) biomes.

Table S1 A summary of species information used in this study.

Figure Legends

Figure 1 Phylogenetic tree of 73 species from across various functional groups and climates-of-origin (see details in Supporting Information Table S1) and its maximum plant night time stomatal conductance (g_{sn}).

Figure 2 (a) Relationship between species' maximum plant night time stomatal conductance (g_{sn}) and mean of annual precipitation (MAP). Regression lines represent univariate relationships rather than the output of the full model and are for visualization purposes only. **(b)** Mean decrease in accuracy (%IncMSE, mean and standard deviation) estimated from 1000 simulations of random forests in evaluating the importance of native climate, represented by mean, on g_{sn} . Native climate variables are annual mean temperature (AMT), mean temperature of warmest quarter (MTW), annual precipitation (MAP), precipitation of driest quarter (PDQ) and vapor pressure deficit of driest quarter (VDQ). Soil organic carbon (SOC) is represented as an approximation to native soil nutrient conditions.

Figure 3 Relationship between species' maximum plant night time stomatal conductance (g_{sn}) and its native climate and soil nutrients (soil organic carbon, SOC) estimated from hierarchical Bayesian models. **(a)** Phylogenetic signal (Pagel's λ , mean and 95% CIs) for g_{sn} ($n = 73$). **(b, c)** Standardized coefficient estimates (effective posterior means and 95% CIs) for the effects of native climate, represented by mean **(b)** and median **(c)**, on g_{sn} ($n = 73$). Values reflect standardised data and can be interpreted as relative effect sizes. Native climate variables are annual mean temperature (AMT), mean temperature of warmest quarter (MTW), annual precipitation (MAP), precipitation of driest quarter (PDQ) and vapor pressure deficit of driest quarter (VDQ). Soil organic carbon (SOC) is represented as an approximation to native soil nutrient conditions.

Figure 4 Box and whisker plots of maximum plant night time stomatal conductance (g_{sn}) among different life forms **(a)** and climate zones **(b)** without accounting for possible effects of shared evolutionary history (phylogenetics). Standardized coefficient values (means and 95% CIs) for differences in g_{sn} between different life forms **(c)** and climate zones **(d)** estimated from hierarchical Bayesian models. Life forms are trees, shrubs, grasses, and forbs. Climate zones are boreal (Bo), temperate dry (TeD), and temperate wet (TeW). In box and whisker plots, the horizontal lines and ranges represent median, first quartile, and third quartile of g_{sn} . In hierarchical Bayesian models, values reflect standardised data and can be interpreted as relative effect sizes.

